Article

Single-Chain Magnet (NEt)[Mn(5-MeOsalen)Fe(CN)] Made of Mn–Fe–Mn Trinuclear Single-Molecule Magnet with an *S* = / Spin Ground State

Marilena Ferbinteanu, Hitoshi Miyasaka, Wolfgang Wernsdorfer, Kazuya Nakata, Ken-ichi Sugiura, Masahiro Yamashita, Claude Coulon, and Rodolphe Clrac

J. Am. Chem. Soc., **2005**, 127 (9), 3090-3099• DOI: 10.1021/ja0468123 • Publication Date (Web): 10 February 2005

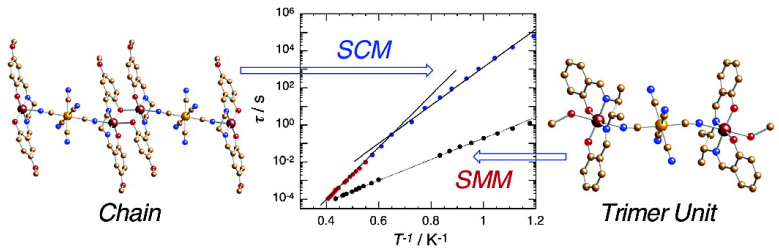

More About This Article

Additional resources and features associated with this article are available within the HTML version:

- Supporting Information
- Links to the 51 articles that cite this article, as of the time of this article download
- Access to high resolution figures
- Links to articles and content related to this article
- Copyright permission to reproduce figures and/or text from this article

View the Full Text HTML

J|A|C|S
ARTICLES
Published on Web 02/10/2005

Single-Chain Magnet $(NEt_4)[Mn_2(5\text{-}MeOsalen)_2Fe(CN)_6]$ Made of $Mn^{III}-Fe^{III}-Mn^{III}$ Trinuclear Single-Molecule Magnet with an $S_T = {}^9/_2$ Spin Ground State

Marilena Ferbinteanu,[†,#] Hitoshi Miyasaka,*[,†,‡] Wolfgang Wernsdorfer,[§] Kazuya Nakata,[†] Ken-ichi Sugiura,[†] Masahiro Yamashita,[†,¶,#] Claude Coulon,[£] and Rodolphe Clérac*[,£]

Contribution from the Department of Chemistry, Graduate School of Science, Tokyo Metropolitan University, 1-1 Minami-ohsawa, Hachioji, Tokyo 192-0397, Japan, PRESTO, Japan Science and Technology Agency (JST), 4-1-8 Honcho Kawaguchi, Saitama 332-0012, Japan, Laboratoire Louis Néel, CNRS, BP 166, 25 Avenue des Martyrs, 38042 Grenoble Cedex 9, France, CREST, JST, 4-1-8 Honcho Kawaguchi, Saitama 332-0012, Japan, and Centre de Recherche Paul Pascal, CNRS UPR 8641, 115 Avenue du Dr. A. Schweitzer, 33600 Pessac, France

Received May 29, 2004; Revised Manuscript Received December 15, 2004; E-mail: miyasaka@comp.metro-u.ac.jp; clerac@crpp-bordeaux.cnrs.fr

Abstract: The cyano-bridged trinuclear compound, $(NEt_4)[Mn_2(salmen)_2(MeOH)_2Fe(CN)_6]$ (**1**) ($salmen^{2-}$ = *rac-N,N′*-(1-methylethylene)bis(salicylideneiminate)), reported previously by Miyasaka et al. (ref 19d) has been reinvestigated using combined ac and dc susceptibility measurements. The strong frequency dependence of the ac susceptibility and the slow relaxation of the magnetization show that **1** behaves as a single-molecule magnet with an $S_T = {}^9/_2$ spin ground state. Its relaxation time (τ) follows an Arrhenius law with $\tau_0 = 2.5 \times 10^{-7}$ s and $\Delta_{eff}/k_B = 14$ K. Moreover, below 0.3 K, τ saturates around 470 s, indicating that quantum tunneling of the magnetization becomes the dominant process of relaxation. $(NEt_4)[Mn_2(5\text{-}MeOsalen)_2Fe(CN)_6]$ (**2**) ($5\text{-}MeOsalen^{2-}$ = *N,N′*-ethylenebis(5-methoxysalicylideneiminate)) is a heterometallic one-dimensional assembly made of the trinuclear $[Mn^{III}(SB)-NC-Fe^{III}-CN-Mn^{III}(SB)]$ (SB is a salen-type Schiff-base ligand) motif similar to **1**. Compound **2** has two types of bridges, a cyano bridge ($-NC-$) and a biphenolate bridge ($-(O)_2-$), connecting Mn^{III} and Fe^{III} ions and the two Mn^{III} ions, respectively. Both bridges mediate ferromagnetic interactions, as shown by modeling the magnetic susceptibility above 10 K with $g_{av} = 2.03$, $J_{Mn-Fe}/k_B = +6.5$ K, and $J'/k_B = +0.07$ K, where J' is the exchange coupling between the trimer units. The dc magnetic measurements of a single crystal using micro-SQUID and Hall-probe magnetometers revealed a uniaxial anisotropy ($D_T/k_B = -0.94$ K) with an easy axis lying along the chain direction. Frequency dependence of the ac susceptibility and time dependence of the dc magnetization have been performed to study the slow relaxation of the magnetization. A mean relaxation time has been found, and its temperature dependence has been studied. Above 1.4 K, both magnetic susceptibility and relaxation time are in agreement with the dynamics described in the 1960s by R. J. Glauber for one-dimensional systems with ferromagnetically coupled Ising spins ($\tau_0 = 3.7 \times 10^{-10}$ s and $\Delta_1/k_B = 31$ K). As expected, at lower temperatures below 1.4 K, the relaxation process is dominated by the finite-size chain effects ($\tau'_0 = 3 \times 10^{-8}$ s and $\Delta_2/k_B = 25$ K). The detailed analysis of this single-chain magnet behavior and its two regimes is consistent with magnetic parameters independently estimated (J' and D_T) and allows the determination of the average chain length of 60 nm (or 44 trimer units). This work illustrates nicely a new strategy to design single-chain magnets by coupling ferromagnetically single-molecule magnets in one dimension.

Introduction

Besides classical magnets that present a three-dimensional magnetic ordering, some paramagnetic systems have been recently considered as magnets undergoing very slow relaxation of their magnetization that may reach years. Among these systems, two types of materials, namely, single-molecule magnets (SMMs)[1] and single-chain magnets (SCMs),[2] are the current focus for many research groups in the field of molecule-based magnetism. Indeed, the motivation to probe these materi-

[†] Tokyo Metropolitan University.
[‡] PRESTO, JST.
[§] Laboratoire Louis Néel.
[¶] CREST, JST.
[£] Centre de Recherche Paul Pascal.
[#] Current address: (M.F. and M.Y.) Department of Chemistry, Graduate School of Science, Tohoku University, Aramaki-Aza-Aoba, Aoba-ku, Sendai 980-8578, Japan.

(1) (a) Christou, G.; Gatteschi, D.; Hendrickson, D. N.; Sessoli, R. *MRS Bull.* **2000**, 66. (b) Gatteschi, D.; Sessoli, R. *Angew. Chem., Int. Ed.* **2003**, *42*, 268.
(2) Clérac, R.; Miyasaka, H.; Yamashita, M.; Coulon, C. *J. Am.* Chem. Soc. **2002**, *124*, 12837.

10.1021/ja0468123 CCC: $30.25

als has been doped by the idea that they may enable the storage of information at the molecular and nanoscale level and may be used in molecular electronics.[3]

In the early 1990s, SMMs had been discovered in manganese clusters, well-known as the Mn_{12} family,[4] and then in several families of Mn,[5] Fe,[6] Ni,[7] V,[8] Co,[9] or mixed-metal[10] polynuclear complexes. In these systems, slow relaxation of the magnetization is closely associated with their intrinsic properties of a high-spin ground state (S_T), a high uniaxial anisotropy (D), and a small transverse anisotropy.[1] These characteristics create an energy barrier, Δ, lying between "spin-up" ($m_s = +S_T$) and "spin-down" ($m_s = -S_T$) states that must be overcome to reverse the spin direction. Therefore, when a strong magnetic field is applied on this superparamagnetic system, the magnetization saturates and relaxes slowly after shutting down the field. This relaxation is characterized by a relaxation time which follows a thermally activated behavior (Arrhenius law) with an energy gap, Δ.

In the SCM systems, the slow relaxation is induced by the same characteristics as those in the SMM systems (uniaxial anisotropy and high-spin ground state) but also by the ferromagnetic coupling (J) operating between anisotropic high-spin units along the chain.[2] Indeed, in 1963, Glauber predicted the slow relaxation of a one-dimensional system possessing ferromagnetically coupled Ising spins.[11] In this model, the relaxation time followed an activated behavior with an energy barrier of $\Delta_{Glauber} = 8JS_T^2$.[12] Since the first evidence of slow relaxation in a one-dimensional system reported by Caneschi et al. in 2001, only a limited number of SCMs have been reported to date.[2,13−16] Among them, we have reported the first example of a system which can be considered as a chain of ferromagnetically coupled anisotropic spins.[2] This family of SCMs has been synthesized based on $Mn^{III}_2Ni^{II}$, $S_T = 3$, repeating units: $[Mn_2(saltmen)_2Ni(pao)_2(L^1)_2](A)_2$ (saltmen^{2-} = *N*,*N*′-(1,1,2,2-tetramethylethylene)bis(salicylideneiminate); pao$^-$ = pyridine-2-aldoximate; L^1 = pyridine, 4-picoline, 4-*tert*-butylpyridine, or *N*-methylimidazole; and A^- = ClO_4^-, BF_4^-, PF_6^-, or ReO_4^-).[14] Due to its simplicity, this system has offered a unique opportunity to test Glauber's theory and to generalize it to the real case, including finite anisotropy and the finite size of the chains.[17] In our previous papers devoted to this system, we have established that the ferromagnetic arrangement of uniaxial anisotropic units with a high-spin state would be a neat strategy to design SCMs.[2,14,17] From this idea, SMMs are prototype examples of such molecular objects as they are well-known to possess these two characteristics.

Recently, Long et al. reported SMM behavior in the cyano-bridged trimer, $K[Mn_2(5\text{-Brsalen})_2(H_2O)_2Fe(CN)_6]$,[18] which exhibits an $S_T = {}^9/_2$ ground state due to the ferromagnetic coupling between Mn^{III} and Fe^{III} via cyano bridges.[19] At the same time, we have studied this [Mn^{III}(SB)−NC−Fe^{III}−CN−

(3) (a) Wernsdorfer, W.; Sessoli, R. *Science* **1999**, *284*, 133. (b) Leuenberger, M. N.; Loss, D. *Nature* **2001**, *410*, 789.
(4) (a) Boyd, P. D. W.; Li, Q.; Vincent, J. B.; Folting, K.; Chang, H.-R.; Streib, W. E.; Huffman, J. C.; Christou, G.; Hendrickson, D. N. *J. Am. Chem. Soc.* **1988**, *110*, 8537. (b) Caneschi, A.; Gatteschi, D.; Sessoli, R. *J. Am. Chem. Soc.* **1991**, *113*, 5873. (c) Sessoli, R.; Tsai, H.-L.; Schake, A. R.; Wang, S.; Vincent, J. B.; Folting, K.; Gatteschi, D.; Christou, G.; Hendrickson, D. N. *J. Am. Chem. Soc.* **1993**, *115*, 1804.
(5) (a) Aubin, S. M. J.; Wemple, M. W.; Adams, D. M.; Tsai, H.; Christou, G.; Hendrickson, D. N. *J. Am. Chem. Soc.* **1996**, *118*, 7746. (b) Yoo, J.; Brechin, E. K.; Yamaguchi, A.; Nakano, M.; Huffman, J. C.; Maniero, A. L.; Brunel, L.-C.; Awaga, K.; Ishimoto, H.; Christou, G.; Hendrickson, D. N. *Inorg. Chem.* **2000**, *39*, 3615. (c) Yoo, J.; Yamaguchi, A.; Nakano, M.; Krzystek, J.; Streib, W. E.; Brunel, L.-C.; Ishimoto, H.; Christou, G.; Hendrickson, D. N. *Inorg. Chem.* **2001**, *40*, 4604. (d) Boskovic, C.; Brechin, E. K.; Streib, W. E.; Folting, K.; Hendrickson, D. N.; Christou, G. *J. Am. Chem. Soc.* **2002**, *124*, 3725. (e) Brechin, E. K.; Boskovic, C.; Wernsdorfer, W.; Yoo, J.; Yamaguchi, A.; Sanudo, E. C.; Concolino, T.; Rheingold, A. L.; Ishimoto, H.; Hendrickson, D. N.; Christou, G. *J. Am. Chem. Soc.* **2002**, *124*, 9710. (f) Brechin, E. K.; Soler, M.; Davidson, J.; Hendrickson, D. N.; Parsons, S.; Christou, G. *Chem. Commun.* **2002**, 2252. (g) Boskovic, C.; Bircher, R.; Tregenna-Piggott, P. L. W.; Güdel, H. U.; Paulsen, C.; Wernsdorfer, W.; Barra, A.-L.; Khatsko, E.; Neels, A.; Stoeckli-Evans, H. *J. Am. Chem. Soc.* **2003**, *125*, 14046. (h) Miyasaka, H.; Clérac, R.; Wernsdorfer, W.; Lecren, L.; Bonhomme, C.; Sugiura, K.; Yamashita, M. *Angew. Chem., Int. Ed.* **2004**, *43*, 2801. (i) Tasiopoulos, A. J.; Vinslava, A.; Wernsdorfer, W.; Abboud, K. A.; Christou, G. *Angew. Chem., Int. Ed.* **2004**, *43*, 2117. (j) Murugesu, M.; Habrych, M.; Wernsdorfer, W.; Abboud, K. A.; Christou, G. *J. Am. Chem. Soc.* **2004**, *126*, 4766. (k) Soler, M.; Wernsdorfer, W.; Folting, K.; Pink, M.; Christou, G. *J. Am. Chem. Soc.* **2004**, *126*, 2156. (l) Murugesu, M.; Raftery, J.; Wernsdorfer, W.; Christou, G.; Brechin, E. K. *Inorg. Chem.* **2004**, *43*, 4203. (m) Sanudo, E. C.; Wernsdorfer, W.; Abboud, K. A.; Christou, G. *Inorg. Chem.* **2004**, *43*, 4137. (n) Wittick, L. M.; Murray, K. S.; Moubaraki, B.; Batten, S. R.; Spiccia, L.; Berry, K. *J. Chem. Soc., Dalton Trans.* **2004**, 1003.
(6) (a) Delfs, C.; Gatteschi, D.; Pardi, L.; Sessoli, R.; Wieghardt, K.; Hanke, D. *Inorg. Chem.* **1993**, *32*, 3099. (b) Barra, A. L.; Caneschi, A.; Cornia, A.; Fabrizi de Biani, F.; Gatteschi, D.; Sangregorio, C.; Sessoli, R.; Sorace, L. *J. Am. Chem. Soc.* **1999**, *121*, 5302. (c) Gatteschi, D.; Sessoli, R.; Cornia, A. *Chem. Commun.* **2000**, 725. (d) Oshio, H.; Hoshino, N.; Ito, T. *J. Am. Chem. Soc.* **2000**, *122*, 12602. (e) Benelli, C.; Cano, J.; Journaux, Y.; Sessoli, R.; Solan, G. A.; Winpenny, R. E. P. *Inorg. Chem.* **2001**, *40*, 188. (f) Goodwin, J. C.; Sessoli, R.; Gatteschi, D.; Wernsdorfer, W.; Powell, A. K.; Heath, S. L. *J. Chem. Soc., Dalton Trans.* **2000**, 1835. (g) Oshio, H.; Hoshino, N.; Ito, T.; Nakano, M. *J. Am. Chem. Soc.* **2004**, *126*, 8805.
(7) (a) Cadiou, C.; Murrie, M.; Paulsen, C.; Villar, V.; Wernsdorfer, W.; Winpenny, R. E. P. *Chem. Commun.* **2001**, 2666. (b) Andres, H.; Basler, R.; Blake, A. J.; Cadiou, C.; Chaboussant, G.; Grant, C. M.; Güdel, H.-U.; Murrie, M.; Parsons, S.; Paulsen, C.; Semadini, F.; Villar, V.; Wernsdorfer, W.; Winpenny, R. E. P. *Chem.—Eur. J.* **2002**, *8*, 4867. (c) Yang, E.-C.; Wernsdorfer, W.; Hill, S.; Edwards, R. S.; Nakano, M.; Maccagnano, S.; Zakharov, L. N.; Rheingold, A. L.; Christou, G.; Hendrickson, D. N. *Polyhedron* **2003**, *22*, 1727. (d) Moragues-Cánovas, M.; Helliwell, M.; Ricard, L.; Rivière, E.; Wernsdorfer, W.; Brechin, E.; Mallah, T. *Eur. J. Inorg. Chem.* **2004**, 2219.
(8) Castro, S. L.; Sun, Z.; Grant, C. M.; Bollinger, J. C.; Hendrickson, D. N.; Christou, G. *J. Am. Chem. Soc.* **1998**, *120*, 2365.
(9) Yang, E.; Hendrickson, D. N.; Wernsdorfer, W.; Nakano, M.; Zakharov, L. N.; Sommer, R. D.; Rheingold, A. L.; Ledezma-Gairaud, M.; Christou, G. *J. Appl. Phys.* **2002**, *91*, 7382.
(10) (a) Schake, A. R.; Tsai, H.; Webb, R. J.; Folting, K.; Christou, G.; Hendrickson, D. N. *Inorg. Chem.* **1994**, *33*, 6020. (b) Sokol, J. J.; Hee, A. G.; Long, J. R. *J. Am. Chem. Soc.* **2002**, *124*, 7656. (c) Karasawa, S.; Zhou, G.; Morikawa, H.; Koga, N. *J. Am. Chem. Soc.* **2003**, *125*, 13676. (d) Choi, H. J.; Sokol, J. J.; Long, J. R. *Inorg. Chem.* **2004**, *43*, 1606. (e) Osa, S.; Kido, T.; Matsumoto, N.; Re, N.; Pochaba, A.; Mrozinski, J. *J. Am. Chem. Soc.* **2004**, *126*, 420. (f) Zaleski, C. M.; Depperman, E. C.; Kampf, J. W.; Kirk, M. L.; Pecoraro, V. L. *Angew. Chem., Int. Ed.* **2004**, *43*, 3912. (g) Miyasaka, H.; Nezu, T.; Sugimoto, K.; Sugiura, K.; Yamashita, M.; Clérac, R. *Chem.—Eur. J.* In press.
(11) (a) Glauber, R. J. *J. Math. Phys.* **1963**, *4*, 294. (b) Susuki, M.; Kubo, R. *J. Phys. Soc. Jpn.* **1968**, *24*, 51.
(12) In ref 11a, the energy barrier, $\Delta_{Glauber}$, is equal to 4J based on the following Hamiltonian: $H = -J\sum_i \sigma_i\sigma_{i+1}$ with $\sigma_i = \pm 1$. In this paper, we have used $H = -2J\sum_i S_{Tzi}S_{Tz(i+1)}$, which is equivalent with Glauber's notation to $H = -2JS_T^2\sum_i \sigma_i\sigma_{i+1}$. Therefore, with this Hamiltonian definition, the energy gap, $\Delta_{Glauber}$, is $8JS_T^2$.
(13) (a) Caneschi, A.; Gatteschi, D.; Lalioti, N.; Sangregorio, C.; Sessoli, R.; Venturi, G.; Vindigni, A.; Rettori, A.; Pini, M. G.; Novak, M. A. *Angew. Chem., Int. Ed.* **2001**, *40*, 1760. (b) Caneschi, A.; Gatteschi, D.; Lalioti, N.; Sessoli, R.; Sorace, L.; Tangoulis, V.; Vindigni, A. *Chem.—Eur. J.* **2002**, *8*, 286. (c) Caneschi, A.; Gatteschi, D.; Lalioti, N.; Sangregorio, C.; Sessoli, R.; Venturi, G.; Vindigni, A.; Rettori, A.; Pini, M. G.; Novak, M. A. *Europhys. Lett.* **2002**, *58*, 771. (d) Bogani, L.; Caneschi, A.; Fedi, M.; Gatteschi, D.; Massi, M.; Novak, M. A.; Pini, M. G.; Rettori, A.; Sessoli, R.; Vindigni, A. *Phys. Rev. Lett.* **2004**, *92*, 207204.
(14) Miyasaka, H.; Clérac, R.; Mizushima, K.; Sugiura, K.; Yamashita, M.; Wernsdorfer, W.; Coulon, C. *Inorg. Chem.* **2003**, *42*, 8203
(15) (a) Chang, F.; Gao, S.; Sun, H.-L.; Hou, Y.-L.; Su, G. Proceedings of the ICSM 2002 Conference; Shanghai, China, 2002. (b) Lescouëzec, R.; Vaissermann, J.; Ruiz-Pérez, C.; Lloret, F.; Carrasco, R.; Julve, M.; Verdaguer, M.; Dromzee, Y.; Gatteschi, D.; Wernsdorfer, W. *Angew. Chem., Int. Ed.* **2003**, *42*, 1483. (c) Toma, L. M.; Lescouëzec, R.; Lloret, F.; Julve, M.; Vaissermann, J.; Verdaguer, M. *Chem. Commun.* **2003**, 1850. (d) Pardo, E.; Ruiz-Garcia, R.; Lloret, F.; Faus, J.; Julve, M.; Journaux, Y.; Delgado, F.; Ruiz-Perez, C. *Adv. Mater.* **2004**, *16*, 1597.
(16) (a) Liu, T.; Fu, D.; Gao, S.; Zhang, Y.; Sun, H.; Su, G.; Liu, Y. *J. Am. Chem. Soc.* **2003**, *125*, 13976. (b) Shaikh, N.; Panja, A.; Goswami, S.; Banerjee, P.; Vojtsek, P.; Zhang, Y.-Z.; Su, G.; Gao, S. *Inorg. Chem.* **2004**, *43*, 849. (c) Wang, S.; Zuo, J.-L.; Gao, S.; Song, Y.; Zhou, H.-C.; Zhang, Y.-Z.; You, X.-Z. *J. Am. Chem. Soc.* **2004**, *126*, 8900. (d) Chakov, N. E.; Wernsdorfer, W.; Abboud, K. A.; Christou, G. *Inorg. Chem.* **2004**, *43*, 5919.
(17) Coulon, C.; Clérac, R.; Lecren, L.; Wernsdorfer, W.; Miyasaka, H. *Phys. Rev. B* **2004**, *69*, 132408.
(18) Choi, H. J.; Sokol, J. J.; Long, J. R. *Inorg. Chem.* **2004**, *43*, 1606.

Chart 1

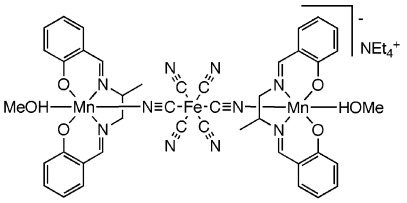

$(NEt_4)[Mn_2(salmen)_2(MeOH)_2Fe(CN)_6]$ (**1**)

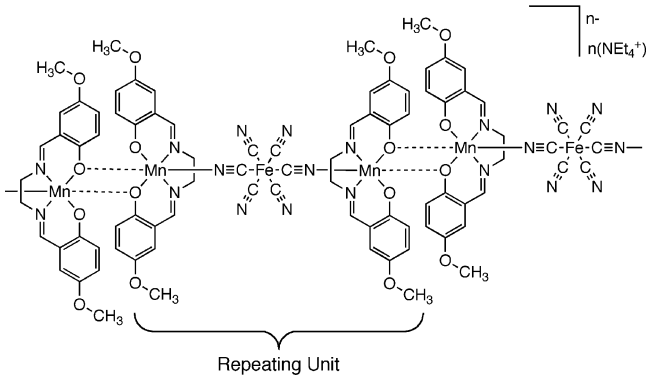

$(NEt_4)[Mn_2(5\text{-}MeOsalen)_2Fe(CN)_6]$ (**2**)

$Mn^{III}(SB)]$ motif (SB is a salen-type Schiff-base ligand) and used it as a building unit to design new SCMs. As a first step, the low-temperature magnetism of $K[Mn_2(5\text{-}Brsalen)_2(H_2O)_2\text{-}Fe(CN)_6]$ has been studied using ac magnetic measurements lacking in our previous report.[19b] Unfortunately, we have been unable to observe any SMM behavior. Consequently, the weak ac signal observed in ref 18 is probably coming from byproducts or crystalline defects. Nevertheless, we have reinvestigated the magnetic properties of a second $[Mn^{III}(SB)-NC-Fe^{III}-CN-Mn^{III}(SB)]$ trimer, $(NEt_4)[Mn_2(salmen)_2(MeOH)_2Fe(CN)_6]$ (**1**) ($salmen^{2-}$ = *rac*-*N*,*N*′-(1-methylethylene)bis(salicylideneiminate)),[19d] and we will report in the present paper its unambiguous SMM properties. Using this encouraging result, we have synthesized a one-dimensional assembly made of ferromagnetically coupled $[Mn^{III}(SB)-NC-Fe^{III}-CN-Mn^{III}(SB)]$ trimers with an $S_T = {}^9/_2$ spin state, $(NEt_4)[Mn_2(5\text{-}MeOsalen)_2Fe(CN)_6]$ (**2**) ($5\text{-}MeOsalen^{2-}$ = *N*,*N*′-ethylenebis(5-methoxysalicylideneiminate)) (Chart 1). This compound exhibits slow relaxation of the magnetization, i.e. SCM behavior, and will be compared to the SMM properties of the trinuclear unit. A detailed analysis of these relaxation processes will be described in this paper.

Experimental Section

General Procedures and Materials. All chemicals and solvents used in the syntheses were reagent grade. Syntheses of the starting materials, $[Mn(5\text{-}MeOsalen)(H_2O)]PF_6$ and $(Et_4N)_3[Fe(CN)_6]$, have been performed according to literature methods.[20,21] $(NEt_4)[Mn_2(salmen)_2\text{-}(MeOH)_2Fe(CN)_6]$ (**1**) was prepared as described elsewhere.[19d]

Synthesis of 2. At room temperature, a methanol solution (30 mL) of $[Mn(5\text{-}MeOsalen)(H_2O)]PF_6$ (0.271 g, 0.5 mmol) was added to a methanol solution (20 mL) of $(Et_4N)_3[Fe(CN)_6]$ (0.3 g, 0.5 mmol). After stirring for several minutes, the mixture was filtered. The filtrate was then kept in the dark for 1 week at room temperature to form brown−black crystals of **2**. Yield: 83%. Anal. Calcd for $C_{50}H_{56}N_{11}O_8Mn_2Fe$ (M = 1104.78): C, 54.36; H, 5.11; N, 13.95. Found: C, 54.36; H, 5.10; N, 13.95. IR (KBr) (ν/cm^{-1}): 1613, 1635 (C═N), 2102 (terminal C≡N), 2112 (bridge C≡N).

Physical Measurements. Infrared spectra were measured on a KBr disk with a Shimadzu FT-IR-8600 spectrophotometer. Magnetic susceptibility measurements were obtained with the use of a Quantum Design SQUID magnetometer (MPMS-XL). The dc measurements were conducted from 1.8 to 300 K and from −70 to 70 kOe. The ac measurements were performed at frequencies ranging from 1 to 1500 Hz with an ac field amplitude of 3 Oe and no dc field applied. The measurements were performed on finely ground polycrystalline samples restrained by Nujol. Experimental data were also corrected for the sample holder, Nujol, and for the diamagnetic contribution calculated from Pascal constants.[22] Magnetization measurements on single crystals were performed with an array of micro-SQUIDs.[23] This magnetometer works in the temperature range of 0.04−7 K and in fields of up to 0.8 T with sweeping rates as high as 0.28 T/s, along with field stability better than microtesla. The time resolution is approximately 1 ms. The field can be applied in any direction of the micro-SQUID plane with precision much better than 0.1° by separately driving three orthogonal coils. To ensure good thermalization, a single crystal was fixed with Apiezo grease. Transverse field magnetization measurements were performed with a home-built Hall probe magnetometer. The Hall probes (typically 10 × 10 μm^2) are made of two-dimensional GaAs/GaAsAl heterostructures and work in the temperature range of 1.5−100 K and in magnetic fields of up to 16 T.

Crystallography. A single crystal of **2** was prepared according to the method described in the synthetic procedure. The single crystal, having dimensions of 0.15 × 0.08 × 0.05 mm^3, was mounted on a glass rod. Data collection was made on a Rigaku CCD diffractometer (Saturn 70) with graphite monochromated Mo Kα radiation (λ = 0.71069 Å). The structures were solved by heavy-atom Patterson methods[24] and expanded using Fourier techniques.[25] Non-hydrogen atoms were refined anisotropically, whereas hydrogen atoms were introduced as fixed contributors. The final cycle of full-matrix least-squares refinements on F^2 was based on 4356 observed reflections and 368 variable parameters and converged with the unweighted, and weighted agreement factors of $R1 = \Sigma||F_o| - |F_c||/\Sigma|F_o|$ and $wR2 = [\Sigma w(F_o^2 - F_c^2)^2/\Sigma w(F_o^2)^2]^{1/2}$ were used ($w = 1/[0.0019F_o^2 + 1.0000\sigma_c\text{-}(F_o^2)]/(4F_o^2)$). A Sheldrick weighting scheme was used. Plots of $\Sigma w(F_o^2 - F_c^2)^2$ versus F_o^2, the reflection order in data collection, sin θ/λ, and various classes of indices showed no unusual trends. Neutral atom scattering factors were taken from Cromer and Waber.[26] Anomalous dispersion effects were included in F_{calcd}; the values of $\Delta f'$ and $\Delta f''$ were those of Creagh and McAuley.[27] The values of the mass attenuation coefficients were those of Creagh and Hubbel.[28] All calculations were performed using the CrystalStructure crystallographic software package.[29] The crystal data and details of the structure

(19) (a) Miyasaka, H.; Matsumoto, N.; Okawa, H.; Re, N.; Gallo, E.; Floriani, C. *Angew. Chem., Int. Ed. Engl.* **1995**, *34*, 1446. (b) Miyasaka, H.; Matsumoto, N.; Okawa, H.; Re, N.; Gallo, E.; Floriani, C. *J. Am. Chem. Soc.* **1996**, *118*, 981. (c) Miyasaka, H.; Matsumoto, N.; Re, N.; Gallo, E.; Floriani, C. *Inorg. Chem.* **1997**, *36*, 670. (d) Miyasaka, H.; Ieda, H.; Matsumoto, N.; Re, N.; Crescenzi, R.; Floriani, C. *Inorg. Chem.* **1998**, *37*, 25. (e) Miyasaka, H.; Okawa, H.; Miyazaki, A.; Enoki, T. *J. Chem. Soc., Dalton Trans.* **1998**, 3991.
(20) Kennedy, B. J.; Murray, K. S. *Inorg. Chem.* **1985**, *24*, 1552.
(21) Mascharak, P. K. *Inorg. Chem.* **1986**, *25*, 245.
(22) Boudreaux, E. A.; Mulay, L. N. *Theory and Applications of Molecular Paramagnetism*; John Wiley & Sons: New York, 1976.
(23) Wernsdorfer, W. *Adv. Chem. Phys.* **2001**, *118*, 99.
(24) Beurskens, P. T.; Admiraal, G.; Beurskens, G.; Bosman, W. P.; Garcia-Granda, S.; Gould, R. O.; Smits, J. M. M.; Smykalla, C. *DIRDIF*; Technical Report of the Crystallography Laboratory; University of Nijmengen: The Netherlands, 1992.
(25) *DIRDIF94*; Beurskens, P. T.; Admiraal, G.; Beurskens, G.; Bosman, W. P.; de Gelder, R.; Israel, R.; Smits, J. M. M. University of Nijmengen: The Netherlands, 1994.
(26) Cromer, D. T.; Waber, J. T. *International Tables for Crystallography*; The Kynoch Press: Birmingham, England, 1974; Vol. 4, Table 2.2A.
(27) Creagh, D. C.; McAuley, W. J. *International Tables for Crystallography*; Wilson, A. J. C., Ed.; Kluwer Academic Publishers: Boston, 1992; Vol. C, Table 4.2.6.8, pp 219−222.

Table 1. Crystallographic Data for **2**

formula	$C_{50}H_{56}N_{11}O_8Mn_2Fe$
formula weight	1104.78
color, shape	brown, prism
crystal system	triclinic
space group	$P-1$ (No. 2)
T/K	117(1)
a/Å	9.877(3)
b/Å	11.162(4)
c/Å	12.536(5)
α/°	87.32(2)
β/°	70.98(2)
γ/°	74.77(2)
V/Å^3	1259.6(8)
Z	1
D_{calc}/g·cm^{-3}	1.456
F_{000}	573.00
No. of reflections	12264
No. of observations	4356
No. of variables	368
μ (Mo Kα)/cm^{-1}	8.42
GOF	1.003
$R1^a(I > 2.00\sigma(I))$	0.052
$R1^a$ (all data)	0.078
$wR2^b$ (all data)	0.148

^{a} $R1 = \sum||F_o| - |F_c||/\sum|F_o|$. ^{b} $wR2 = [\sum w(F_o^2 - F_c^2)^2/\sum w(F_o^2)^2]^{1/2}$.

Table 2. Selected Bond Distances (Å) and Angles (deg) for **2** with the Estimated Standard Deviations in Parentheses

distance	(Å)	angle	(deg)
Mn(1)−O(1)	1.913(3)	O(1)−Mn(1)−O(3)	96.0(1)
Mn(1)−O(3)	1.870(2)	O(1)−Mn(1)−N(1)	89.3(1)
Mn(1)−N(1)	1.985(3)	O(1)−Mn(1)−N(2)	167.6(1)
Mn(1)−N(2)	1.990(4)	O(1)−Mn(1)−N(3)	95.9(1)
Mn(1)−N(3)	2.179(3)	O(1)−Mn(1)−O(1)^a	81.4(1)
Mn(1)−O(1)^a	2.375(3)	O(3)−Mn(1)−N(1)	172.8(2)
Fe(1)−C(19)	1.916(3)	O(3)−Mn(1)−N(2)	91.7(1)
Fe(1)−C(20)	1.954(5)	O(3)−Mn(1)−N(3)	96.2(1)
Fe(1)−C(21)	1.951(5)	O(3)−Mn(1)−O(1)^a	91.4(1)
C(19)−N(3)	1.153(4)	N(1)−Mn(1)−N(2)	82.3(1)
C(20)−N(4)	1.157(6)	N(1)−Mn(1)−N(3)	87.9(1)
C(21)−N(5)	1.160(7)	N(1)−Mn(1)-O(1)^a	84.6(1)
Mn(1)···Mn(1)^a	3.2644(8)	N(2)−Mn(1)−N(3)	92.8(1)
		N(2)−Mn(1)−O(1)^a	88.7(1)
		N(3)−Mn(1)−O(1)^a	172.1(1)
		Mn(1)−O(1)−Mn(1)^a	98.6(1)
		Mn(1)−N(3)−C(19)	146.7(4)
		N(3)−C(19)−Fe(1)	176.3(5)
		N(4)−C(20)−Fe(1)	177.8(3)
		N(5)−C(21)−Fe(1)	178.3(3)
		C(19)−Fe(1)−C(20)	91.6(2)
		C(19)−Fe(1)−C(21)	91.9(2)
		C(20)−Fe(1)−C(21)	89.3(2)

^{a} Symmetry operation: $-x - 1, -y + 1, -z$.

determination of **2** are summarized in Table 1. Selected bond distances and angles are listed in Table 2.

Results and Discussion

Synthesis. Single crystals of **1** have been prepared using the procedure described previously.[19d] The compound is very stable in air due to the absence of crystallization solvent molecules. Moreover, the apical methanol molecules capping the discrete trinuclear structure as (Chart 1) are eliminated only above 105 °C. In theory, this type of trinuclear unit could be "polymerized" into a one-dimensional assembly due to the affinity of the Mn^{III}-(SB) complex to form an out-of-plane dimeric motif via a biphenolate bridge (this would be achieved by the elimination of the capping solvents). Indeed, this scenario has been experimentally observed in the family of $[Mn_2(saltmen)_2$-

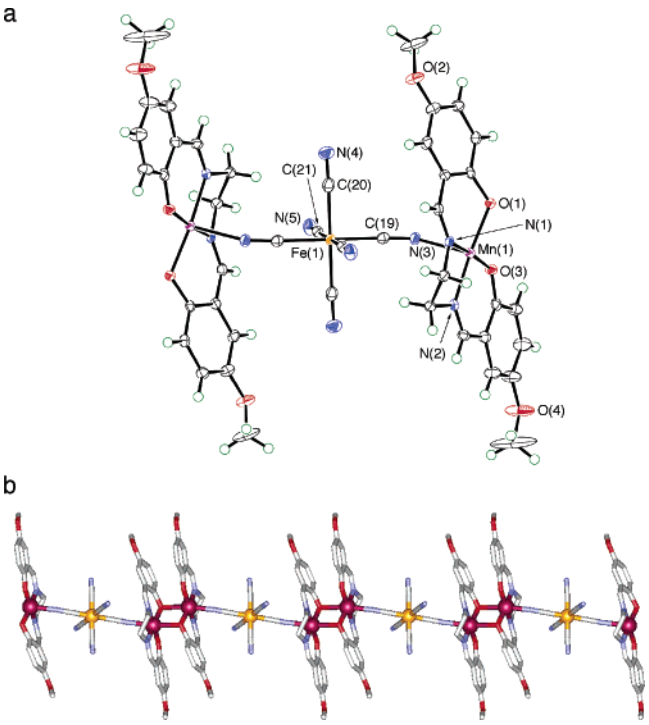

Figure 1. (a) View of the Mn^{III}−Fe^{III}−Mn^{III} trinuclear monoanionic unit in **2** with the atom numbering scheme of the unique atoms (50% probability ellipsoid). This motif is reminiscent of the trinuclear compound **1**. (b) One-dimensional assembly of Mn^{III}−Fe^{III}−Mn^{III} trinuclear units in **2**.

$Ni(pao)_2(L^1)_2](A)_2$[2,14] and also in **2**. Compound **2** was selectively synthesized as crystals in high yield (83%) by the assembly reaction of $[Mn(5\text{-MeOsalen})(H_2O)]PF_6$ with $(Et_4N)_3[Fe(CN)_6]$ in methanol at room temperature. The assemblies of Mn^{III} salen-type compounds with hexacyanometalate(III) have been widely studied to date,[19,30] but one-dimensional assembly has been only seen in $(Et_4N)_2[Mn(acacen)][Fe(CN)_6]$ ($acacen^{2-}$ = *N*,*N*′-ethylenebis(acetylacetonylideneaminato)) showing a 1:1 alternating arrangement of Fe^{III} and Mn^{III}.[31] Considering that the same 1:1 stoichiometric conditions have been used for $(Et_4N)_2$-$[Mn(acacen)][Fe(CN)_6]$ (1:1 chain),[31] **1** (trinuclear compound),[19d] and **2** (1:2 chain, vide infra), the final structural arrangement of the assembly compounds is thus strongly dependent on the packing effects tuned by the employed type of salen ligands and counterions.

Structural Description. The structure of **1** has been described in detail in ref 19d and will not be further described in this paper.

As shown in Figure 1a, the basic unit of **2** is composed of two $[Mn(5\text{-MeOsalen})]^+$ parts and one $[Fe(CN)_6]^{3-}$ moiety, forming a cyano-bridged linear-like trinuclear unit [Mn−NC−Fe−CN−Mn]. Each terminal $[Mn(5\text{-MeOsalen})]^+$ part is further

(28) Creagh, D. C.; Hubbell, J. H. *International Tables for Crystallography*; Wilson, A. J. C., Ed.; Kluwer Academic Publishers: Boston, 1992; Vol. C, Table 4.2.4.3, pp 200−206.
(29) *CrystalStructure 3.15*, Crystal Structure Analysis Package; Rigaku and Rigaku/MSC: The Woodlands, TX, 2000−2002.
(30) (a) Miyasaka, H.; Okawa, H.; Miyazaki, A.; Enoki, T. *Inorg. Chem.* **1998**, *37*, 4878. (b) Miyasaka, H.; Ieda, H.; Matsumoto, N.; Sugiura, K.; Yamashita, M. *Inorg. Chem.* **2003**, *42*, 3509. (c) Clemente-León, M.; Coronado, E.; Galán-Mascarós, J. R.; Gómez-García, C. J.; Woike, T.; Clemente-Juan, J. M. *Inorg. Chem.* **2001**, *40*, 87. (d) Przychodzén, P.; Lewinski, K.; Balanda, M.; Pelka, R.; Rams, M.; Wasiutynski, T.; Guyard-Duhayon, C.; Sieklucka, B. *Inorg. Chem.* **2004**, *43*, 2967.
(31) Re, N.; Gallo, E.; Floriani, C.; Miyasaka, H.; Matsumoto, N. *Inorg. Chem.* **1996**, *35*, 6004.

linked and forms an out-of-plane dimer with the corresponding moiety of adjacent trimer units. Consequently, a one-dimensional chain is obtained with a $[-(O)_2-Mn-NC-Fe-CN-Mn]$ repeating unit (Figure 1b). The $[Fe(CN)_6]^{3-}$ acts as *trans*-bridge between two $[Mn_2(5\text{-MeOsalen})_2]^{2+}$ dimer units with a bending angle of C(19)−N(3)−Mn(1) = 146.7(4)°. This feature is generally seen in compounds having a −CN−Mn(R-salen)−NC− bridging mode (137−170 °).[18,19,30,32] In the trimer compound **1**, the corresponding angle is 164.7(9)° slightly more linear than that in **2**.[19d] The Fe^{III} ion occupies the inversion center (Figure 1a). Its octahedral coordination sphere is slightly compressed along the chain axis (Fe(1)−C(19) = 1.916(3)) in comparison to the other directions: Fe(1)−C(20) = 1.954(5) and Fe(1)−C(21) = 1.951(5) Å. As expected for Mn^{III} ions, a Jahn−Teller distortion is observed and induces a strongly distorted square bipyramidal geometry around the Mn^{III} site with an elongated axis along the N(3)−Mn(1)−O(1)* direction (N(3)−Mn(1) = 2.179(3) and Mn(1)−O(1)* = 2.375(3) Å; symmetry operation (*), $-x-1, -y+1, -z$). It is worth noting that the Jahn−Teller axis is parallel to the chain direction. The equatorial plane of the Mn^{III} site is occupied by the 5-MeOsalen ligand with average distances of <Mn−N> = 1.988 Å and <Mn−O> = 1.892 Å. Similar geometry around the Mn site has been observed in **1** with $N_{CN}-Mn$ = 2.219(9) Å and $O_{MeOH}-Mn$ = 2.422(7) Å.[19d]

As described above, **2** is made of anionic chains running in the ($a-b$) direction (Figure 2a). NEt_4^+ cations are located between the chains leading to a shortest interchain metal−metal distance of 11.16 Å. Moreover, no significant interchain interactions, such as $\pi-\pi$ stacking or hydrogen bonding, are observed between 5-MeOsalen ligands or dangling −CN groups of neighboring chains (Figure 2b).

Single-Molecule Magnet Behavior in 1. In the previous study of the magnetic properties of **1**,[19d] the ferromagnetic interaction between Fe^{III} and Mn^{III} was estimated at +5.2 K leading to an $S_T = {}^9/_2$ ground state. Nevertheless, the low-temperature magnetic properties of this compound have not been reported in the literature. In the present work, the low-temperature behavior of **1** has been investigated in detail in order to probe the anisotropic nature of this trinuclear motif. Below 7 K, the field dependence of the magnetization was measured on an oriented single crystal applying the field along the *b* axis (Figures S1 and 3). This orientation corresponds to the easy axis of the crystal and also to a direction only at 19° of the local easy axes of the four trinuclear complex orientations. Below 1.1 K (Figure 3), hysteresis loops are observed in the easy direction, and they become temperature independent below 0.5 K, staying however, field sweep-rate dependent even at 0.04 K (Figure S2). This result highlights the slow relaxation of the magnetization and suggests that **1** behaves as a SMM. Analyzing these hysteresis loops in more detail, we observe two steps due to fast relaxation processes at 0.04 K. The step close to zero field, at ±40 mT (H_{ex}), corresponds to the fast relaxation between the two lower-energy levels, $m_S = \pm{}^9/_2$. This relaxation expected at zero field is slightly shifted due to weak antiferromagnetic intercomplex interactions which can be estimated to a maximum value of −5 mK ($|J'| = g\mu_B H_{ex}/(2S_T)$). Around $\mu_0 H_1 = 1$ T, a second fast relaxation is observed corresponding

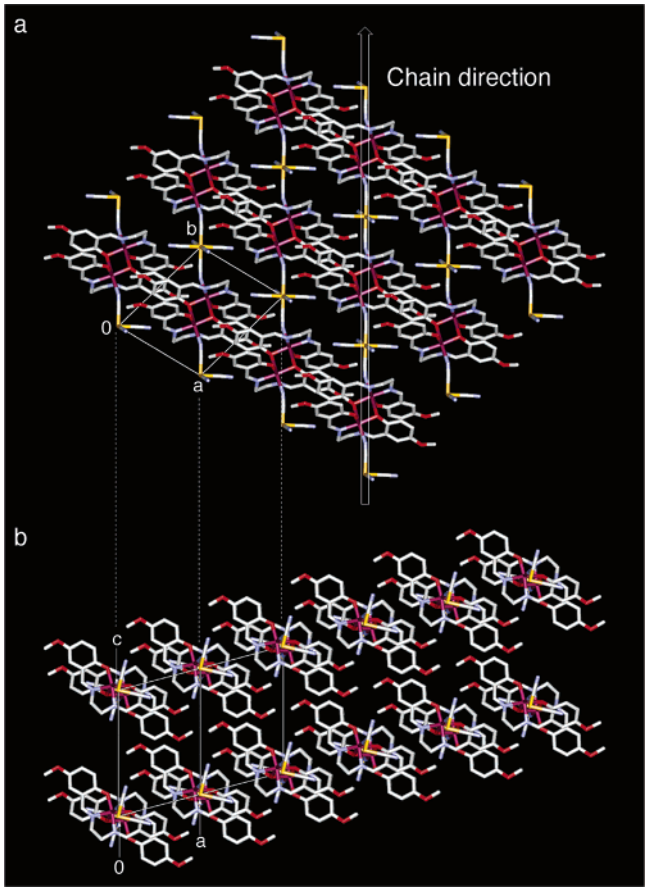

Figure 2. Packing diagrams of **2**. (a) Projection along the *c* axis showing the chains running along the ($a-b$) direction. (b) Projection along the chain axis. Tetraethylammonium cations located between chains have been omitted for clarity.

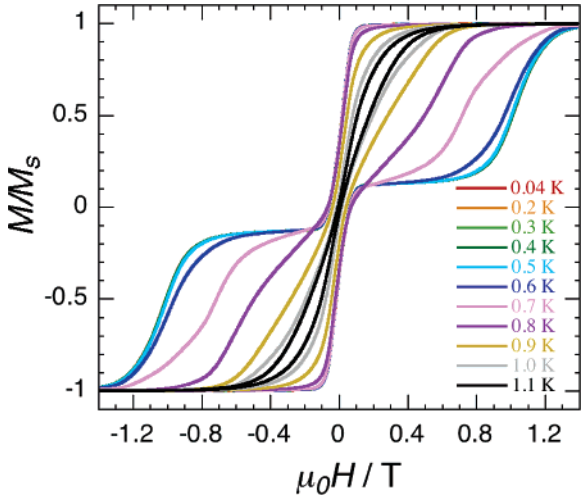

Figure 3. Field dependence of the magnetization below 1.1 K on an oriented single crystal of **1** along the *b* axis with a sweep field rate of 0.07 T/s.

to the first crossing between two energy levels (i.e., $m_S = {}^9/_2$ and $-{}^7/_2$). From this H_1 field, the uniaxial anisotropy, D_T, of the trinuclear compound can be estimated at −1.3 K ($|D_T| = g\mu_B H_1$, using $g = 2$). It should be noted that this value is in good agreement with the value ($D_T/k_B = -1.22$ K) estimated from the fitting of the reduced magnetization (Figure S3). To study the slow relaxation of the magnetization, two techniques have been performed: (i) ac susceptibility measurements (as a

(32) (a) Matsumoto, N.; Sunatsuki, Y.; Miyasaka, H.; Hashimoto, Y.; Luneau, D.; Tuchagues, J.-P. *Angew. Chem., Int. Ed.* **1999**, *38*, 171. (b) Kim, Y.; Park, S.-M.; Nam, W.; Kim, S.-J. *Chem. Commun.* **2001**, 1470.

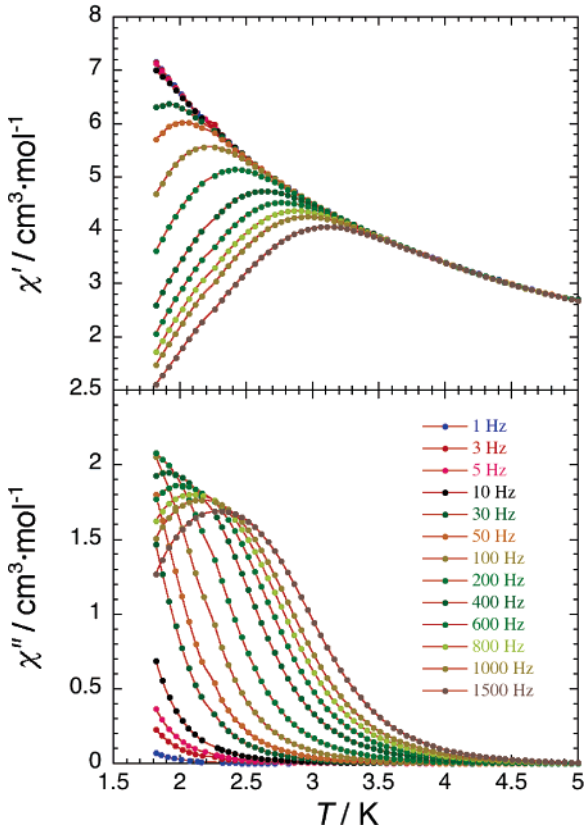

Figure 4. Temperature dependence of the real (χ') and imaginary (χ'') parts of the ac susceptibility for **1** measured under various oscillating frequencies (1−1500 Hz). The solid lines are a guide for the eyes.

function of the temperature and the frequency), and (ii) direct measurements of the magnetization decay.

Figures 4 and S4 show temperature and frequency dependences of the ac susceptibility for **1**, where χ' is the in-phase susceptibility and χ'' is the out-of-phase susceptibility. Below 5 K, χ' and χ'' are strongly frequency dependent, confirming the slow relaxation of the magnetization. Between 2.5 and 1.82 K, the relaxation time (τ) was deduced from the maximum of the $\chi''(T)$ and $\chi''(\nu)$ curves (red dots in Figure 5). Below 1.82 K, the relaxation time becomes too slow to be studied with ac measurements in the available range of frequencies. Therefore, direct measurements of the magnetization relaxation were performed down to 0.04 K (Figure S5). In agreement with the field dependence of the magnetization (Figure 3), the relaxation process becomes temperature independent below 0.5 K, suggesting a regime where the relaxation is only possible via quantum tunneling of the magnetization. This feature is characteristic of the SMM behavior, as already observed in other systems.[5a,7a,33] All the $M/M_s(t)$ curves can be scaled into a single master curve. The relaxation time, τ, was extracted at each temperature taking $\tau = t$ when $M/M_s(t)$ reaches $1/e$ (blue dots in Figure 5). Above 1 K, the relaxation time follows an Arrhenius law (Figure 5):

$$\tau(T) = \tau_0 \exp(\Delta_{eff}/(k_B T)) \qquad (1)$$

with $\tau_0 = 2.5 \times 10^{-7}$ s and $\Delta_{eff}/k_B = 14$ K, where τ_0 is the pre-exponential factor and k_B is the Boltzmann constant. In SMM systems, the theoretical energy barrier (Δ) can be estimated from $\Delta = |D|S_T^2$ for integer spins or $\Delta = |D|(S_T^2 - {}^1/_4)$ for half-integer spins. Using an average value of D_T (−1.25 K) obtained from the above data, the theoretical energy gap should be 25 K, although the experimental value only reaches 14 K. This effective reduction of the energy gap has also been observed in other SMM systems.[5a,h] Different reasons have been invoked to explain its reduction, among them the fact that quantum tunneling is operative even in the Arrhenius regime or that low-lying excited states of the SMM complex short cut the energy gap. Below 1 K, the relaxation time deviates from the linear dependence and saturates at 470 s below 0.5 K, as expected when quantum tunneling becomes the dominant process of relaxation in a SMM.[5a,7a,33]

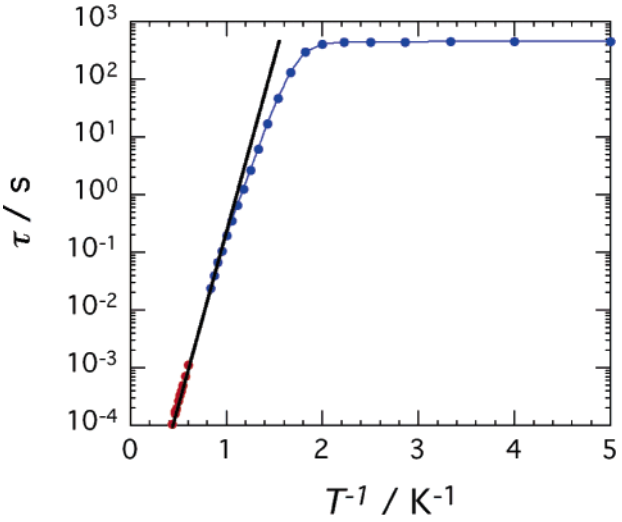

Figure 5. Relaxation time (τ) versus $1/T$ for **1** deduced from ac measurements (red dots) and from dc measurements (blue dots). The black solid line is the least-squares fit of the data above 1 K with an Arrhenius law, with $\tau_0 = 2.5 \times 10^{-7}$ s and $\Delta_{eff}/k_B = 14$ K (see text).

In conclusion, the combined ac and dc measurements gathered at low temperatures on **1** indicate unambiguously its SMM behavior induced by a high-spin ground state, $S_T = {}^9/_2$, and a strong uniaxial anisotropy, $D_T/k_B = -1.25$ K.

High-Temperature Magnetic Behavior of 2: Intrachain Magnetic Interactions. The dc magnetic measurements were carried out on a polycrystalline sample of **2** in the temperature range from 300 to 1.8 K at an external field of 0.1 T. At temperatures above 30 K, the temperature dependence of the susceptibility obeys a Curie−Weiss law with $C = 6.63$ $cm^3 \cdot K \cdot mol^{-1}$ and $\theta = 7.6$ K. The obtained Curie constant is in good agreement with the predicted spin-only value, that is, 6.38 $cm^3 \cdot K \cdot mol^{-1}$ for two Mn^{III} ($S = 2$) and one Fe^{III} ($S = {}^1/_2$), assuming an average g value of 2.0. The positive sign of the Weiss constant indicates that the dominant interactions are ferromagnetic. Therefore, as expected when decreasing temperature (Figure 6), the χT versus T curve is increasing gradually from 6.8 $cm^3 \cdot K \cdot mol^{-1}$ at 300 K to reach a maximum of 49.0 $cm^3 \cdot K \cdot mol^{-1}$ at 2.2 K (followed by a slight decrease to 46.0 $cm^3 \cdot K \cdot mol^{-1}$ at 1.82 K).

On the basis of the structural description, two different exchange couplings can be identified along the chain: (i) a $Mn^{III} \cdots Fe^{III}$ interaction, J_{Mn-Fe}, via a cyano bridge, and (ii) a $Mn^{III} \cdots Mn^{III}$ exchange, J_{Mn-Mn}, via a biphenolate bridge.

(33) (a) Sangregorio, C.; Ohm, T.; Paulsen, C.; Sessoli, R.; Gatteschi, D. *Phys. Rev. Lett.* **1997**, *78*, 4645. (b) Aubin, S. M. J.; Dilley, N. R.; Pardi, L.; Krzystek, J.; Wemple, M. W.; Brunel, L.-C.; Maple, M. B.; Christou, G.; Hendrickson, D. N. *J. Am. Chem. Soc.* **1998**, *120*, 4991.

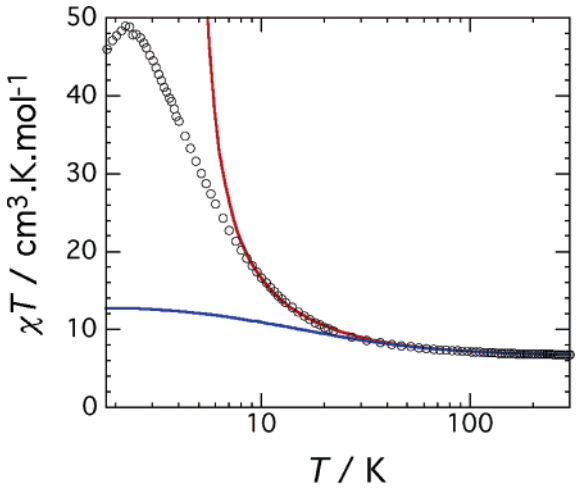

Figure 6. Temperature dependence of the χT product at 0.1 T measured on a polycrystalline sample of **2**. Solid red and blue lines correspond to the simulations with a trimer model, respectively, with and without taking into account intrachain intertrimer magnetic interactions in the mean-field approximation (see text).

Reading the literature on related systems, we expect both interactions to be ferromagnetic. The J_{Mn-Fe} value ranges from +3 to +8.5 K for very similar systems, including Mn−NC−Fe bridges, like in **1**[19d] or other discrete compounds.[18,19] The magnetic interaction, J_{Mn-Mn}, mediated by a biphenolate bridge between two Mn^{III} is also expected to be ferromagnetic, and its magnitude ranges from +0.2 to +2.6 K.[5h,34−36] Nevertheless, in the one-dimensional compounds obtained with this similar out-of-plane dimeric motif ($[Mn_2(saltmen)_2Ni(pao)_2(L^1)_2](A)_2$),[2,14] J_{Mn-Mn} always ranges below +1.4 K.

Hence, a first approach to simulate the magnetic susceptibility was performed based on a Heisenberg trinuclear model with the spin system (S_{Mn}, S_{Fe}, $S_{Mn} = 2, {}^1/_2, 2$) and considering J_{Mn-Mn} to be smaller than J_{Mn-Fe}. The following Heisenberg Hamiltonian was used assuming an external magnetic field (H) along the z axis ($H = H_z$):

$$H = -2J_{Mn-Fe}(S_{Mn1}S_{Fe} + S_{Mn1A}S_{Fe}) + g_{av}\mu_B S_{Tz}H_z \quad (2)$$

where S_T is the total spin operator of the trimer with $S_T = S_{Mn1} + S_{Fe} + S_{Mn1A}$; S_{Tz} is the z component of the S_T operator, and g_{av} is the Landé factor assuming $g_{av} = g_{Mn} = g_{Fe}$. The diagonalization of the Hamiltonian leads to nine different eigenvalues (E_i), and in the low-field limit ($\mu_B H/k_B T \ll 1$), an analytical expression of the susceptibility can be obtained.[37] As shown in Figure 6 (blue line), this model was unable to reproduce correctly the susceptibility below 30 K ($J_{Mn-Fe}/k_B = +8.5$ K and $g_{av} = 2.03$). Therefore, intrachain intertrimer interactions, J', have been introduced in the frame of the mean-field approximation.[38] Considering the experimental data above 10 K, the best set of parameters obtained using this model are $J_{Mn-Fe}/k_B = +6.5$ K, $zJ'/k_B = +0.14$ K, and $g_{av} = 2.03$ (red line in Figure 6). It is worth noticing that the amplitude of the magnetic interaction, J_{Mn-Fe}, falls remarkably in the range given in the literature (*vide supra*).[18,19] Considering $J_{Mn-Fe} \gg J'$, this one-dimensional system can be viewed at low temperatures as a chain of ferromagnetic-coupled $S_T = {}^9/_2$ units. It should be noted that the anisotropy of the system has been neglected in the magnetic model, and therefore, the magnetic interaction values and especially J' could be slightly changed taking into account this contribution.

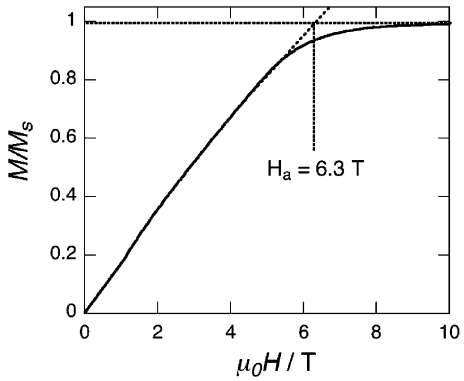

Figure 7. Field dependence of the normalized magnetization (M/M_s) as a function of a magnetic field applied perpendicular to the chain direction (in the hard plane), measured on a single crystal of **2** at 1.5 K.

Low-Temperature Field Dependence of the Magnetization: Anisotropy and Slow Relaxation. When the field dependence of the magnetization of **2** was measured on a polycrystalline sample, no significant hysteresis effects have been observed above 1.8 K (Figure S6). At this temperature, the magnetization value is almost saturated at 7 T, reaching 7.8 μ_B, which is clearly consistent with the ferromagnetic coupling scheme deduced from the high-temperature fitting of the susceptibility (theoretical value of 9 μ_B with $g = 2$). Nevertheless, a total saturation of the magnetization is still not observed even at 7 T, which suggests the presence of a strong anisotropy as that observed in related SCMs[2,14,15d,16ab,17] and in the trinuclear compound **1**. To study this anisotropy, single-crystal measurements have been performed using micro-SQUID and Hall probe techniques. The easy axis of the crystal was found along the chain direction ($a-b$). The plane perpendicular to the chain axis is almost isotropic, as expected for a uniaxial anisotropy, and can be therefore considered as a hard plane. In this plane, the field dependence of the magnetization has been measured up to 10 T (Figure 7). At 1.5 K, the magnetization increases linearly to saturate around 6.3 T (H_a). From this characteristic field, the anisotropy parameter D_T for the $S_T = {}^9/_2$ trimer unit can be deduced by minimizing the sum of the Zeeman and anisotropy energies: $2|D_T|S_T^2 = g\mu_B S_T H_a$. Therefore, D_T is estimated at −0.94 K, in good agreement with the

(34) Miyasaka, H.; Nezu, T.; Sugimoto, K.; Sugiura, K.; Yamashita, M.; Clérac, R. *Inorg. Chem.* **2004**, *43*, 5486.
(35) Miyasaka, H.; Clérac, R.; Ishii, T.; Chang, H.; Kitagawa, S.; Yamashita, M. *J. Chem. Soc., Dalton Trans.* **2002**, 1528.
(36) (a) Sato, Y.; Miyasaka, H.; Matsumoto, N.; Okawa, H. *Inorg. Chim. Acta* **1996**, *247*, 57. (b) Matsumoto, N.; Okawa, H.; Kida, S.; Ogawa, T.; Ohyoshi, A. *Bull. Chem. Soc. Jpn.* **1989**, *62*, 3812. (c) Shyu, H.-L.; Wei, H.-H.; Wang, Y. *Inorg. Chim. Acta* **1999**, *290*, 8.

(37) The Van Vleck equation is:

$$\chi = \frac{N\sum_{i=1}^{n}\left(g\mu_B m_{si}\right)^2 exp\left(-E_i^{(0)}/k_BT\right)}{k_BT\sum_{i=1}^{n}exp\left(-E_i^{(0)}/k_BT\right)}$$

where $E_i^{(0)}$ is the energy of the i state in zero field and N the number of trimers. Then an analytical expression of the magnetic susceptibility can be proposed:

$$\chi_{trimer} = \frac{Ng^2\mu_B^2}{4k_BT}\frac{\left(e^{\frac{-6J}{k_BT}}+e^{\frac{-4J}{k_BT}}\right)+10\left(e^{\frac{-7J}{k_BT}}+e^{\frac{-3J}{k_BT}}\right)+35\left(e^{\frac{-8J}{k_BT}}+e^{\frac{-2J}{k_BT}}\right)+84\left(e^{\frac{-9J}{k_BT}}+e^{\frac{-J}{k_BT}}\right)+165}{\left(e^{\frac{-6J}{k_BT}}+e^{\frac{-4J}{k_BT}}\right)+2\left(e^{\frac{-7J}{k_BT}}+e^{\frac{-3J}{k_BT}}\right)+3\left(e^{\frac{-8J}{k_BT}}+e^{\frac{-2J}{k_BT}}\right)+4\left(e^{\frac{-9J}{k_BT}}+e^{\frac{-J}{k_BT}}\right)+5}$$

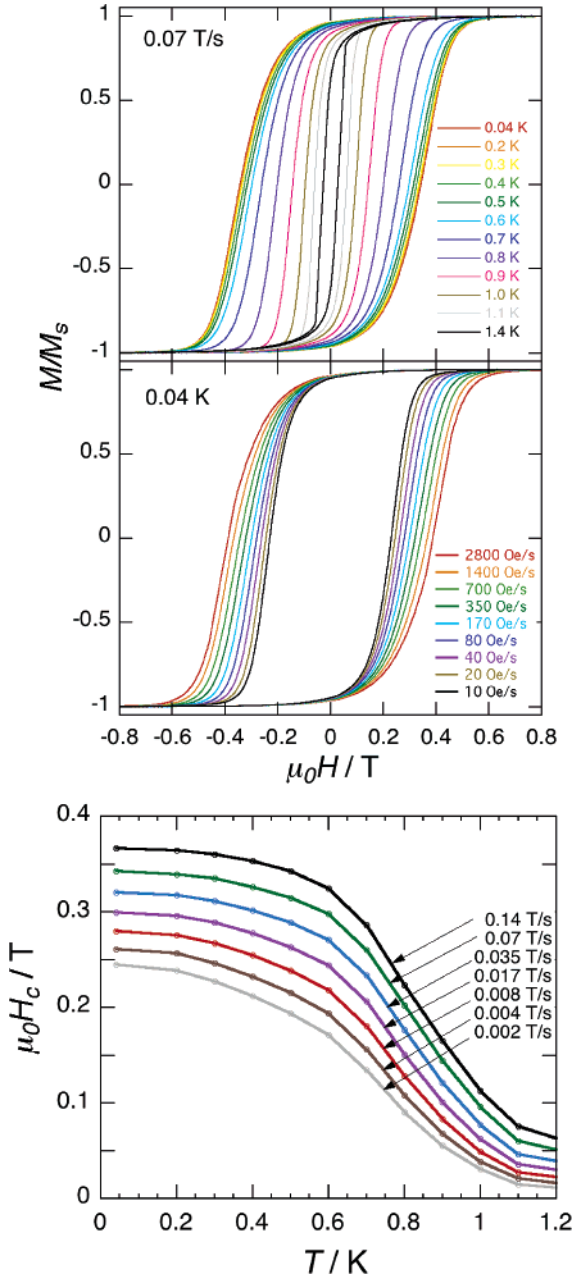

Figure 8. Field dependence of the normalized magnetization (M/M_s) measured on a single crystal of **2** along the easy axis of magnetization (chain direction). Hysteresis loops (top) measured at various temperatures with 0.07 T/s field sweep rate and at 0.04 K at different field sweep rates, and (bottom) temperature and field sweep rate dependences of the coercive field, H_c.

deduced value ($D_T/k_B = -1.25$ K) for **1**, taking into account that the small difference between the two values may be induced by slight geometrical variations (e.g., the C−N−Mn angle is modified from 164.7° in **1** to 146.7° in **2**).

In the easy-axis direction, the magnetization exhibits a rapid saturation and hysteresis effects below 1.4 K, a signature of a "magnet-type" behavior (Figure 8). Even at the lowest accessible temperature (0.04 K), the hysteresis loops are strongly dependent on the field sweep rate (Figure 8). Moreover, at a given sweep rate, the obtained coercive field increases with lowering temperature (from 1.4 to 0.3 K) and finally tends to saturate below 0.3 K (bottom part of Figure 8). This is expected when the magnetization relaxation is dominated by a temperature-

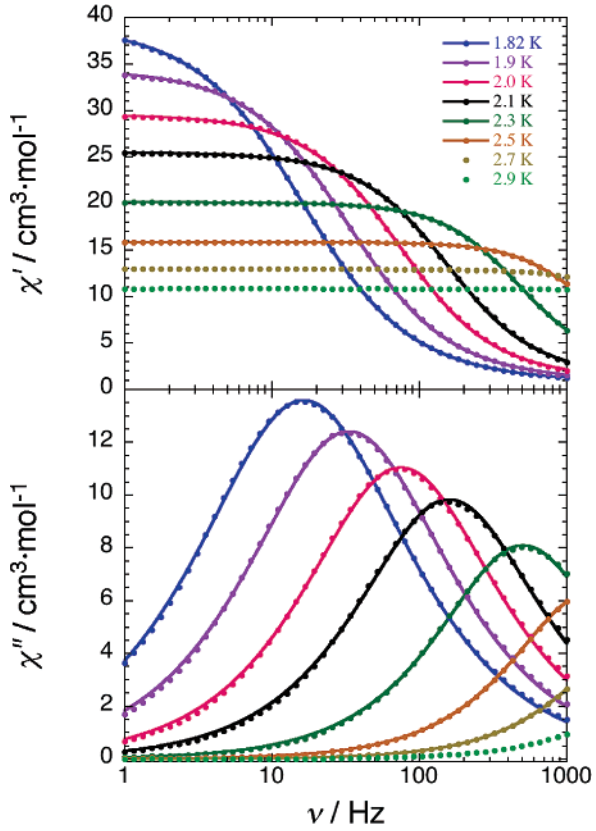

Figure 9. Frequency dependence of the real (χ') and imaginary (χ'') parts of the ac susceptibility for **2** measured between 1.82 and 2.9 K. The solid lines are the best fits obtained with the generalized Debye model. All data have been well simulated with small α values of less than 0.06.

independent process. This tendency of the saturation was also observed in two previous SCM systems[14,16d] and is also reminiscent of the behavior observed in SMM when the quantum tunneling becomes the dominant pathway for the relaxation. More detailed investigations of quantum tunneling and quantum effects in SCM are currently being performed and will be presented elsewhere. To study in more detail the relaxation of the magnetization at zero field in **2**, the associated characteristic time has been measured using combined ac and dc measurements.

Slow Relaxation and Its Characteristic Time (τ). The in-phase (χ') and out-of-phase (χ'') ac susceptibility has been measured as a function of the temperature (below 5 K) and the ac field frequency (ν_{ac} from 1 to 1500 Hz). As illustrated by Figures 9 and S7, both χ' and χ'' are strongly frequency dependent below 3 K. This behavior already observed in SMMs and SCMs as a signature of the magnetization slow relaxation clearly precludes the stabilization of a three-dimensional magnetic order. At a given frequency (ν_{ac}), the energy given to the system by the thermal bath is not enough to let the magnetization (M) follow the applied oscillating field, which hence becomes frozen below the so-called blocking temperature

(38) Using the mean-field approximation to treat the intrachain intertrimer interactions, the following definition of the susceptibility has been used:

$$\chi = \frac{\chi_{trimer}}{1 - \frac{2zJ'}{Ng^2\mu_B^2}\chi_{trimer}}$$

For example, see: (a) Myers, B. E.; Berger, L.; Friedberg, S. *J. Appl. Phys.* **1969**, *40*, 1149. (b) O'Connor, C. J. *Prog. Inorg. Chem.* **1982**, *29*, 203.

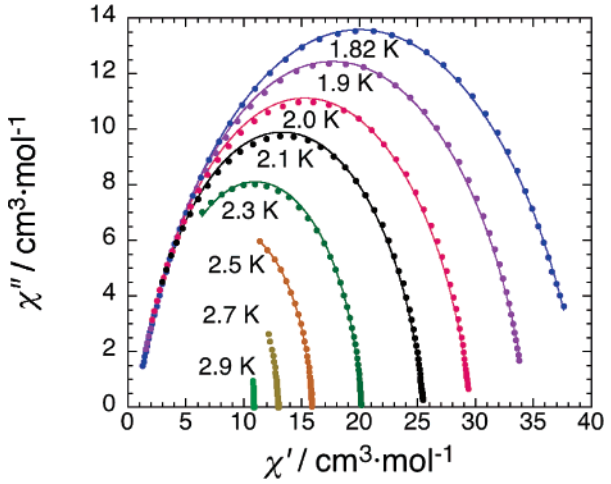

Figure 10. Cole−Cole plots for **2**. The solid lines represent the least-squares fit by a generalized Debye model with $\alpha < 0.06$ (see text).

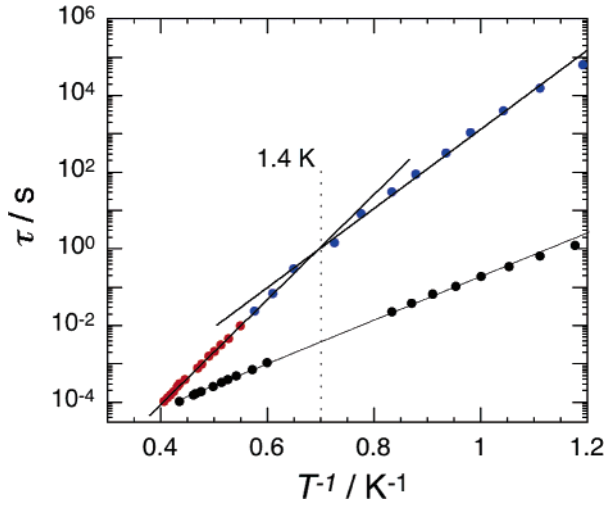

Figure 11. Relaxation time (τ) versus $1/T$ plot for **1** (black dots) and **2** deduced from ac (red dots) and dc (blue dots) measurements.

$T_B(\nu_{ac})$. This blocking process induces the vanishing of the ac response in parallel to the appearance of coercivity. The obtained $\chi'(\nu_{ac})$, $\chi''(\nu_{ac})$, and $\chi''(\chi')$ plots were fitted simultaneously to a generalized Debye model (solid lines in Figures 9 and 10).[14,39]

In the entire temperature range measured, the α parameter quantifying the width of the τ distribution[39a] was found to be always less than 0.06. This result indicates a very narrow distribution of relaxation times, and therefore, a single relaxation time, τ, can be considered. Furthermore, this approximation is also supported by the nearly symmetrical shape of the Cole−Cole plots (Figure 10). Therefore, a single relaxation time, τ, can be deduced from the previous fits and also from the $\chi''(T)$ plots considering that at a given frequency (ν_{ac}), the peak of $\chi''(T)$ is located at the blocking temperature where $\tau(T_B) = 1/(2\pi\nu_{ac})$. As demonstrated by Glauber in 1963,[11] SCM possesses a thermally activated relaxation time (Arrhenius law; eq 1). The semilog plot of τ versus T^{-1} using ac data (red dots in Figure 11) confirms this prediction with $\tau_0 = 3.7 \times 10^{-10}$ s and $\Delta/k_B = 31.1$ K.

(39) (a) Cole, K. S.; Cole, R. H. *J. Chem. Phys.* **1941**, *9*, 341. (b) Boettcher, C. J. F. *Theory of Electric Polarisation*; Elsevier: Amsterdam, 1952. (c) Aubin, S. M.; Sun, Z.; Pardi, L.; Krzysteck, J.; Folting, K.; Brunel, L.-J.; Rheingold, A. L.; Christou, G.; Hendrickson, D. N. *Inorg. Chem.* **1999**, *38*, 5329.

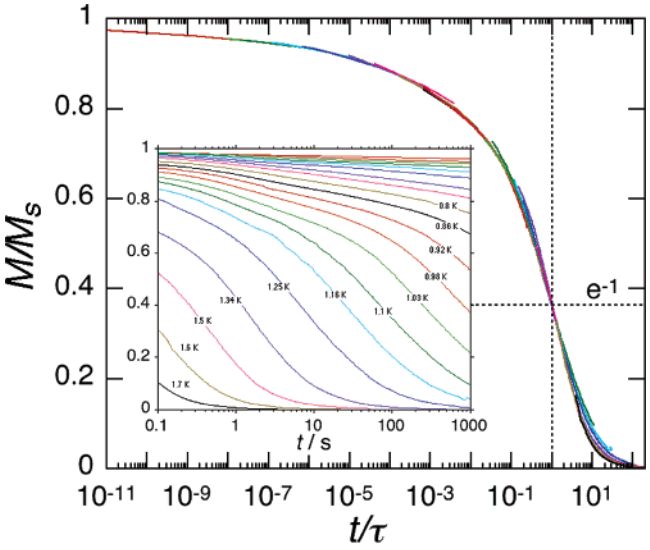

Figure 12. Single-crystal relaxation measurements of **2**: scaling plot of M/M_s versus t/τ. Inset: Single-crystal relaxation measurements of **2** plotted as M/M_s versus t curves.

With our commercial SQUID apparatus, this relaxation time cannot be followed below 1.8 K. Therefore, magnetization decay measurements at lower temperatures down to 0.04 K have been performed on a homemade micro-SQUID magnetometer (Figure 12). The same shape of M/M_s versus t curves (where M/M_s is the magnetization normalized to its saturation value) was obtained for the entire temperature range (inset Figure 12), and therefore, the data were scaled into a single master curve displayed in Figure 12. The relaxation time was extracted by simply taking the time when M/M_s reaches the value $1/e$. It is worth noting that below 0.8 K, the relaxation process becomes too slow, and the estimation of the relaxation time becomes impossible with our techniques. The obtained τ values have been plotted in Figure 11 (blue dots) together with those derived from ac magnetic measurements and the data obtained from the isolated $Mn^{III}-Fe^{III}-Mn^{III}$ $S_T = {}^9/_2$ trimer (**1**). As expected, the thermal variations of the relaxation time observed for **1** and **2** are completely different and attest that the exchange coupling between the SMM trimers dramatically influences the relaxation of the magnetization.

Crossover between Glauber's Relaxation and Finite-Size SCM Regime. Above $T^* = 1.4$ K ($1/T^* = 0.7$ K^{-1}), the relaxation time deduced from the dc measurements is in alignment with the ac data. The fit of the complete set of data above 1.4 K leads to qualitatively the same Arrhenius law as previously obtained ($\tau_0 = 3.7 \times 10^{-10}$ s and $\Delta/k_B = 31$ K). This regime can be relatively well understood generalizing the Glauber theory established for Ising spins to the classical spin model with a finite anisotropy. As demonstrated in ref 17, the relaxation time for an infinite chain of spins with a finite anisotropy (D_T) is $\tau(T) = \tau_0\exp[(8J + |D_T|)S_T^2/(k_BT)]$, where J is the magnetic interaction between $S_T = {}^9/_2$ macrospins. This interaction can be estimated looking at the temperature dependence of the χT product in zero dc field, which is proportional to the correlation length in any one-dimensional classical problem. In a ferromagnetic one-dimensional anisotropic Heisenberg model, this correlation length is exponentially enhanced when lowering the temperature (for any value of D_T)[40] and in the $|D_T| > 4J/3$ Ising limit: $\chi T = C_{eff}\exp(4JS_T^2/k_BT)$.[17] As

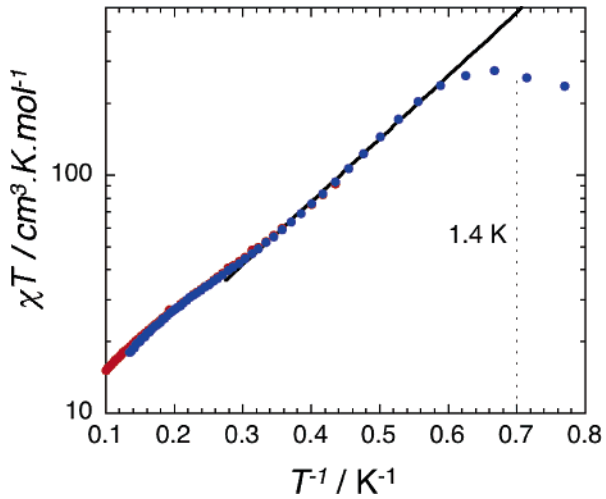

Figure 13. Semilog plot of χT versus $1/T$ for **2** (where χ is the zero-field susceptibility). Red and blue dots have been obtained with ac (0.1 Hz, 0.3 mT of ac field modulation) and dc (numerical derivative of M versus H plots around zero dc field) techniques, respectively.

expected above T^*, Figure 13 shows that $\ln(\chi T)$ versus $1/T$ increases linearly with an energy gap of 6.1 K, which allows an estimation of $J/k_B = +0.08$ K (therefore, $J_{Mn-Mn} = +0.38$ K from $J_{Mn-Mn}/k_B = JS_T^2/S_{Mn}^2$ with $S_T = {}^9/_2$ and $S_{Mn} = 2$). Using this J value together with $D_T/k_B = -0.94$ K, the relaxation time energy gap $\Delta_1/k_B = (8J + |D_T|)S_T^2/k_B$ is 32 K. This value is in excellent agreement with the experimental value and confirms that the slow relaxation of the magnetization is induced by the isolated infinite chain of ferromagnetically coupled anisotropic $S_T = {}^9/_2$ spins. Below 1.4 K, as shown in Figure 11, the relaxation deviates significantly from the previous linear behavior and adopts a second activated regime, with $\tau'_0 = 3 \times 10^{-8}$ s and $\Delta/k_B = 25$ K. This crossover, which has been also observed for $[Mn_2(saltmen)_2Ni(pao)_2(py)_2](ClO_4)_2$,[17] is predicted when the correlation length (ξ) of the ideal infinite chain becomes larger than the real chain length (L)[41] that can be, for example, limited by the structural defects. In this regime when $|D_T| > 4J/3$ (Ising limit relevant in the present case), the relaxation time is also activated.[17] As the relaxation is now dominated by the chain ends ($\xi \geq L$), the correlation part of the energy gap is divided by two: $\tau(T) = \tau'_0\exp[(4J + |D_T|)S_T^2/(k_BT)]$.[17] The low-temperature energy gap, $\Delta_2/k_B = (4J + |D_T|)S_T^2/k_B$, can be estimated from J and D_T at 25.5 K, which is in perfect agreement with the experimental result. A further evidence of this crossover can be obtained looking further at the $\ln(\chi T)$ versus $1/T$ plot (Figure 13). Below T^*, χT saturates at about 300 $cm^3 \cdot K \cdot mol^{-1}$ when the correlation length becomes larger than the real chain length (L). In this limit, the value of saturation is simply equal to nC_{eff}, where C_{eff} and n are the effective Curie constant of the chain defined previously ($C_{eff} = 6.8$ $cm^3 \cdot K \cdot mol^{-1}$) and the number of units in the chain, respectively. Therefore, n can be estimated at 44 and then the chain length at about 60 nm. It should be noted that the estimation of the chain length from T^* ($k_BT^*\ln(2n) = 4JS_T^2$)[17] leads to similar values ($n \approx 40$, $L \approx 55$ nm).

Concluding Remarks

In this paper, the magnetic properties of the trinuclear compound $(NEt_4)[Mn_2(salmen)_2(MeOH)_2Fe(CN)_6]$ (**1**) has been reinvestigated, demonstrating its SMM behavior induced by its $S_T = {}^9/_2$ ground spin state and uniaxial anisotropy. Arranging this trinuclear $[Mn^{III}(SB)-NC-Fe^{III}-CN-Mn^{III}(SB)]$ motif into a one-dimensional assembly, we synthesized and characterized $(NEt_4)[Mn_2(5\text{-}MeOsalen)_2Fe(CN)_6]$ (**2**) structurally and magnetically. On the basis of various dc and ac magnetic measurements, compound **2** can be viewed as a chain of ferromagnetically coupled $S_T = {}^9/_2$ anisotropic macrospins, which exhibits slow relaxation of the magnetization with a single characteristic time. The detailed analysis of the relaxation time and the magnetic susceptibility (or the correlation length) leads consistently to the conclusion that **2** behaves as a SCM. Interestingly, two regimes have been identified: (i) above 1.4 K, since chains in **2** can be considered as infinite ($\xi \ll L$) and introducing a finite anisotropy, the observed relaxation can be understood in the frame of Glauber's theory; (ii) below 1.4 K, since the chain must be viewed as finite objects ($\xi \geq L$), finite-size effects become relevant to describe the relaxation. Although many examples of architectures built from Mn^{III}/salen building blocks and hexacyanometalate are known to date,[18,19,30] the present compound **2** constitutes the first example of the SCM behavior in this family. Moreover, the present results illustrate step by step a new strategy to design single-chain magnets by coupling ferromagnetically single-molecule magnets in one dimension.

Acknowledgment. The authors thank Professor Takayoshi Kuroda-Sowa (Kinki University) for fitting of the reduced magnetization. This work was supported by PRESTO, JST and a Grant-in-Aid for Scientific Research from the Ministry of Education, Culture, Sports, Science, and Technology, Japan (H.M.), CREST, JST (H.M. and M.Y.), and JSPS Research Fellowships for Young Scientists (M.F.). R.C. and C.C. thank the CNRS, the University of Bordeaux 1, and the Conseil Regional d'Aquitaine for a financial support.

Supporting Information Available: Additional magnetic data for **1** and **2** (Figures S1−S7), and X-ray crystallographic file (CIF) for **2**. This material is available free of charge via the Internet at http://pubs.acs.org.

JA0468123

(40) Loveluck, J. M.; Lovesey, S. W.; Aubry, S. *J. Phys. C* **1975**, *8*, 3841.
(41) (a) Leal da Silva, J. K.; Moreira, A. G.; Soares, M. S.; Barreto, F. C. S. *Phys. Rev. E* **1995**, *52*, 4527. (b) Luscombe, J. H.; Luban, M.; Reynolds, J. P. *Phys. Rev. E* **1996**, *53*, 5852.